An Improved ANS Transaction Template

Matthew J. Urffer, L. F. Miller*, A. Mabe†*

Department of Nuclear Engineering, University of Tennessee, Knoxville, TN, 37916
†*Department of Chemistry, University of Tennessee, Knoxville, TN, 37916*
murffer@utk.edu, lfmiller@utk.edu, amabe1@utk.edu

INTRODUCTION

The Department of Homeland Security (DHS) continues to fund research (through the Domestic Nuclear Detection Office (DNDO)) for replacement detectors for nuclear material. These detectors are designed to replace the ^{3}He detectors currently installed as radiation portal monitors. DHS / DNDO (along with PNNL) has determined a set of objectives that replacement technologies should meet (summarized in Table I). These detectors must be able to effectively discriminate between gammas (which can occur in medical isotopes) and neutrons (indicative of special nuclear material).

TABLE I: Replacement Detector Requirements

Parameter	Specification
Absolute neutron detection efficiency	2.5 cps/ng of ^{252}Cf
Intrinsic gamma-neutron detection efficiency	$\epsilon_{int,\gamma n} \leq 10^{-6}$
Gamma absolute rejection ratio for neutrons (GARRn)	$0.9 \leq$ GARRn ≤ 1.1 at 10 mR/h exposure
Cost	\$ 30,000 per system

A possible replacement technology being investigated is ^{6}Li (thermal cross section of 940 barns) embedded in a scintillating polymer matrix. Upon the absorption of a neutron ^{6}Li fissions into two fragments; an alpha particle of energy 2.05 MeV and a triton of energy 2.73 MeV. This large amount of kinetic energy liberated (Q-value 4.78 MeV) makes ^{6}Li an attractive alternative compared to other reactions such as the ^{3}He reaction which has a Q-value of 0.756 MeV or ^{10}B (Q-value of 2.31 MeV). In addition, the the alpha and triton produced are charged ions and relatively easy to stop and detect.

THEORY

Neutron detectors often utilize a material doped with an isotope of large thermal cross section for absorption such as ^{3}He, ^{6}Li or ^{10}B. When these materials absorb a neutron the nucleus of the isotope becomes unstable and fissions into reaction products. These reaction products (having an initial kinetic energy equal to the Q-value of the neutron absorption reaction) travel through the material, transferring their kinetic energy to the material. Photon interactions in the detector occur when a photon scatters off a single electron in a Compton scatter-

ing event and transfers a portion of its energy to the electron predominately through Compton scattering. This Compton electron then produces a cascade of secondary electrons in the material, which, depending upon the energy, may or may not deposit a majority of its energy in the detector. The difference in the transfer of kinetic energy from charged particle to electrons and from photon interactions (Compton scattering) to electrons introduces an opportunity to exploit the difference in energy deposition in order to maximize the discrimination between neutron and photon interactions in a detector.

DESCRIPTION OF WORK

The energy deposition of neutrons and gammas was investigated for polymeric films containing ^{6}Li as ^{6}LiF of thickness ranging from 15 μmto 1 cm. The pulse height spectra of these samples was measured on site at the University of Tennessee's characterization laboratory from a moderated neutron source as wells as a ^{6}Co source. Simulations were completed using GEANT4, a modern toolkit for Monte Carlo transport simulation [1, 2]. The measurements were then used to validate and bench marking the simulation.

Detector Simulation

The detector geometry was simulated as a single layer of neutron absorbing material mounted atop of a non-scintillating material (PMMA). The initial events for runs where chosen by setting up a particle gun for thermal (0.025 eV) neutrons upon the detector and for both gammas resulting from a ^{60}Co decay. The user of the GEANT4 toolkit is responsible for selecting the proper physics processes to model. Thus, extensive use of `G4ModularPhysicsList` was employed to handle the assigning of the physics processes to each particle in the correct order. The physics lists chosen for this simulation are listed below:

- `G4EmStandardPhysics` The electromagnetic physics defines the electrons, muons, and taus along with their corresponding neutrinos. For electrons, the primary concern of this simulation, multiple scattering, electron ionization, and electron bremsstrahlung processes were assigned. In addition the positron is defined and the multiple scattering process, electron ionization process, electron bremsstrahlung process and positron annihilation is assigned.

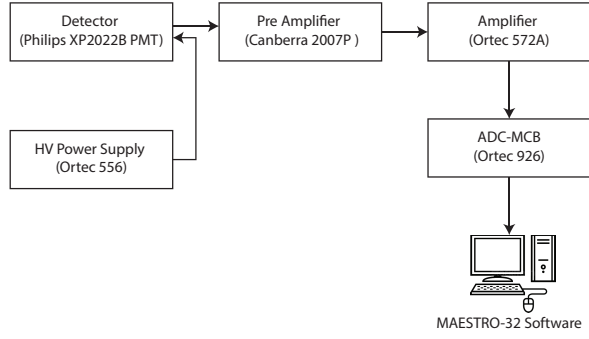- `G4EmLivermorePhysics` The Livermore physics process extend the `EMStandardPhyiscs` down to low (250

Fig. 1: Pulse height measurement electronics

Fig. 2: Simulated Lead and Cadmium Well Spectra. The difference between the two spectra is the thermal neutron response and is what is measured.

eV) energies. The physics processes extended with `G4EmLivermorePhysics` are the photo-electric effect, Compton scattering, Rayleigh scattering, gamma conversion, Ionisation and Bremsstrahlung.

- `HadronPhysicsQGSP_BERT_HP` Hadronic physics are included to model the nuclear interactions. The chosen list is a Quark Gluon String Model for energies in the 5-25 GeV range, with a Bertini cascade model until 20 MeV. Once a hadron has an energy of 20 MeV the high precision cross section driven models are applied.

- `G4IonPhysics` Finally, to handle the transport of the charged ions resulting from an ^{6}Li(n, α)^{3}H interaction the `G4IonPhysics` list was used.

Fabricated Detector Measurements

Samples are mounted to a 10 stage PMT with silicone based optical grease which is attached to a Canberra base (also serving as a preamplifier). The PMT's voltage is supplied by a high voltage power supply, with the power being supplied to the pre amplifier base by an amplifier. The output signal of the C base feeds into the amplifier for pulse shaping and amplification. The amplified signal is then inputed to an MCB-ADC, and can then be read using the MAESTRO-32 software. A schematic of the setup is shown in Figure 1. A 100 μCi ^{Co}60 source was used to measure the gamma energy deposition of the films, while a moderated ^{252}Cf source was used for the neutrons. The ^{252}Cf irridiator contains two detector wells; a lead well and a cadmium well. The lead well measures the response of neutron of all energies, while the cadmium well measures the responses of fast neutrons. The two responses are then subtracted, as shown in Figure 2.

RESULTS

It is well established that the pulse height of a radiation event is proportional to the energy deposition of the event[3]. Thus, the validity of the GEANT4 simulation can be determine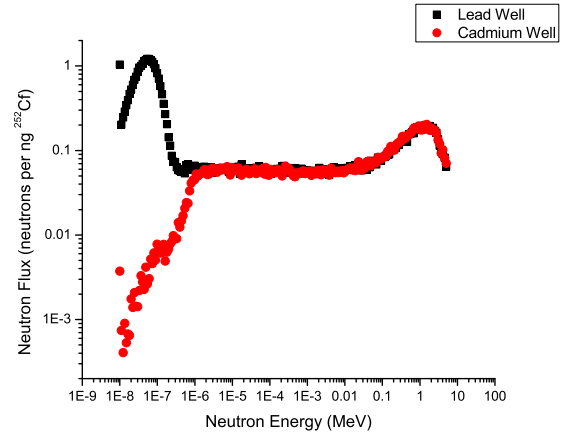d by comparing the spectra shapes of measured spectra to simulated energy deposition. The measured gamma spectra for six polymeric films along with the neutron response of two of the films in Figure 3, while the simulated energy deposition is shown in Figure 4. It is observed that the simulated energy deposition from gammas has the same shape as the measured pulse height spectra (thicker films were not available to be measured), while the pulse height deficit and low energy resolution of the films make a comparison of the neutron spectra difficult. A more quantitative approach was taken for validation by computing the average energy deposition and pulse height, the results of which are shown in Figure 5. With the average energy deposition on the left axis and the average light yield (pulse height) on the right axis, it is possible to compare the measurement and the simulation and agreement is observed.

CONCLUSIONS AND FUTURE WORK

The energy deposition for neutrons and gammas was calculated in thin polymeric films of thickness from 15 μmto 1 cm with the GEANT4 toolkit and compared to the measured spectra. The average energy deposited was computed for each thickness and and normalized by the incident energy for gammas or the Q-value of the reaction for neutrons, and is presented in Table II. Future work will be focused on utilizing the GEANT4 toolkit to explore the energy deposition mechanisms in thin films, focusing on secondary electrons and their ranges. In addition, light transport in layered thin film detectors will be explored.
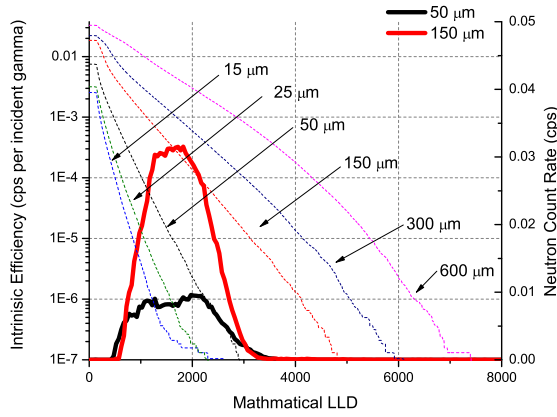
ACKNOWLEDGMENTS

Fig. 3: Gamma intrinsic efficiency (dashed lines) plotted against neutron counts (solid). The gamma spectra has been normalized by the number of incident photons upon the sample, while the neutron spectra has not.

TABLE II: Fractional Energy Deposition for Various Thickness

Thickness	Gamma Fraction	Neutron Fraction
15 μm	0.010	0.531
25 μm	0.013	0.634
50 μm	0.017	0.782
150 μm	0.032	0.927
300 μm	0.052	0.964
600 μm	0.087	0.982
1 mm	0.130	0.989
1 cm	0.425	0.998

views of DNDO.

REFERENCES

1. S. Agostinelli, J. Allison, K. Amako, and et al., "Geant4âĂŤa simulation toolkit," *Nuclear Instruments and Methods in Physics Research Section A: Accelerators, Spectrometers, Detectors and Associated Equipment*, vol. 506, pp. 250–303, July 2003.
2. J. Allison, K. Amako, J. Apostolakis, and et al., "Geant4 developments and applications," *Nuclear Science, IEEE Transactions on*, vol. 53, pp. 270–278, Feb. 2006.
3. J. B. Birks, "Scintillations from organic crystals: Specific fluorescence and relative response to different radiations," *Proceedings of the Physical Society. Section A*, vol. 64, pp. 874–877, Oct. 1951.
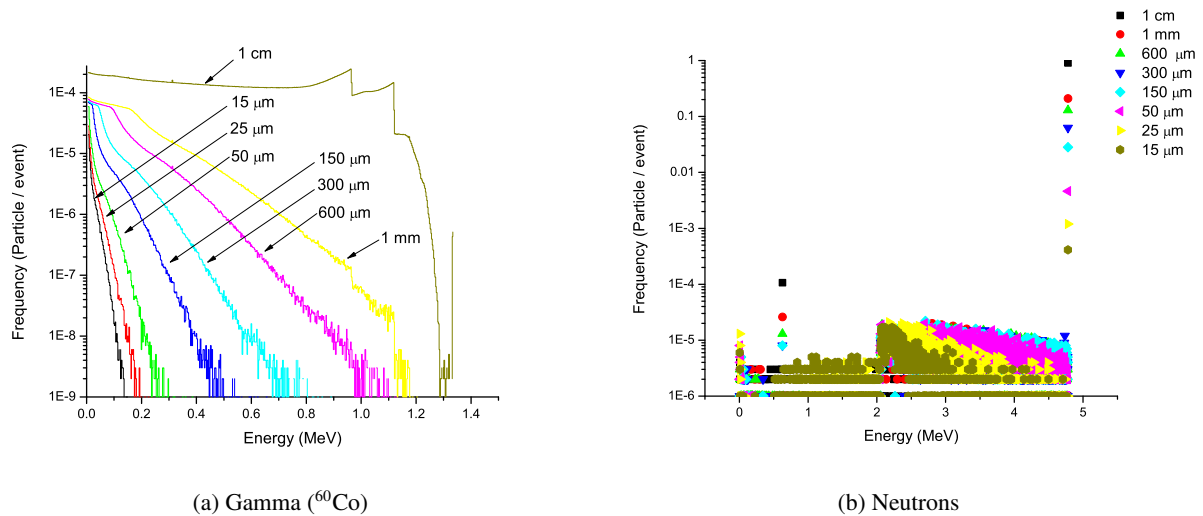
(a) Gamma (^{60}Co)

(b) Neutrons

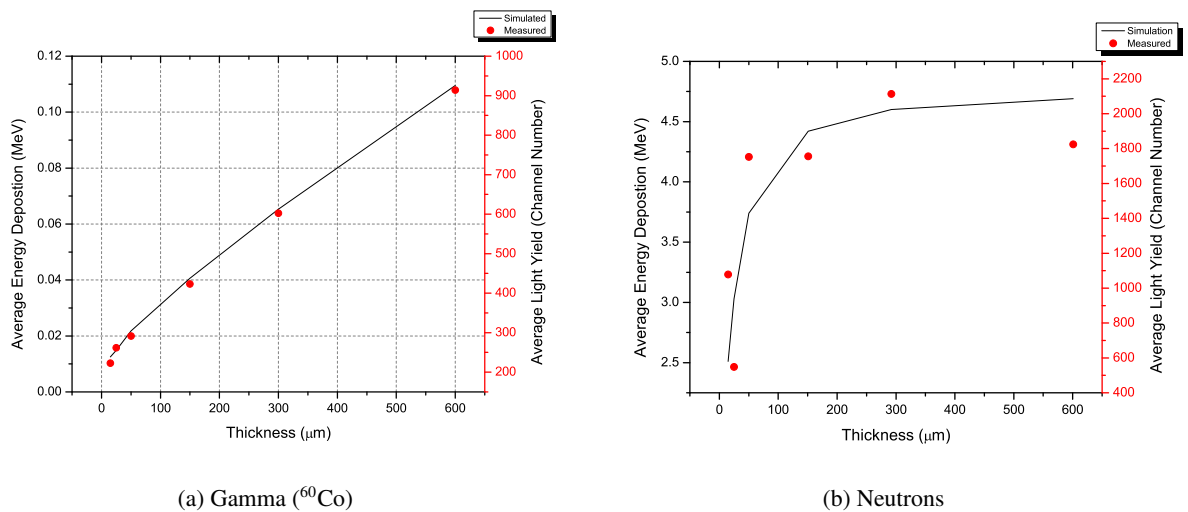Fig. 4: Simulated Energy Deposition

(a) Gamma (^{60}Co)

(b) Neutrons

Fig. 5: Average Energy Deposition and Measured Light Yield